

## Dielectric and Mechanical Absorption Mechanisms for Time and Frequency Domain Transducer Modeling

D. J. Powell, J. Mould and G. L. Wojcik,  
Weidlinger Associates Inc, Los Altos, CA 94022

**Abstract** - In all practical transduction systems—such as biomedical imaging arrays, underwater sonar systems or piezoelectric actuators and transformers, electro-mechanical losses impact overall system performance. Adverse effects of these losses include heat generation, sub-optimal electrical matching, and reduced operational efficiency. Consequently, it is imperative to fully understand the implications of loss mechanisms and incorporate them properly in numerical and analytical models. In this paper, time-domain electromechanical absorption mechanisms are studied in terms of their physical mechanisms and frequency-domain counterparts. We examine the mechanical and dielectric losses of some common piezoelectric materials and discuss some of the issues that arise in attempting to measure and model them.

### INTRODUCTION - WHY MODEL LOSSES?

To accurately model an electromechanical transduction system, using finite element analysis or otherwise, requires the full set of electromechanical properties for each of the system's constituent materials. These properties include stiffness, density, dielectric and piezoelectric coupling constants. Furthermore, the dynamic response of such a system will only be accurately characterized if the model accounts for the loss mechanisms present within each constituent material. These loss mechanisms, primarily mechanical attenuation and dielectric loss, greatly impact a device's efficiency, maximum drive-level (thermal considerations) and resonant characteristics i.e. bandwidth.

In many devices, the losses in the piezoceramic parts of the device are low compared to those in its passive components (matching layers, backing block, filler materials) and radiation losses. Consequently, the resonant characteristics of the device as a whole are dominated by the loss mechanisms in its passive components. However, there are certain applications where the losses within the piezoceramic may pose significant design challenges. For example, in biomedical imaging arrays, the dielectric loss in the piezoceramic is responsible for a significant increase in the transducer's resistance at its electrical resonance

frequency,  $f_E$ . Under extended use with a high pulse repetition frequency (PRF), electrical dissipation in this resistive component results in undesirable heat generation. Strict regulatory limits require that the temperature at the transducer's front face be kept below stringent specified levels. Consequently, great care must be taken during the design process to ensure that these thermal considerations are satisfied.

In the above example, heat generation was undesirable due to regulatory limits and optimal electrical efficiency was not a primary design goal. In the portable computer market however, reduced weight and extended battery life (improved electrical efficiency) are major selling points. Consequently, piezoelectric transformers are finding increased application in the portable computer market where they are used to provide a compact means of producing the high voltages required for fluorescent back lighting etc. These piezoelectric transformers are typically "high Q" devices, made from piezoceramics such as PZT8 with few additional external mechanical components. As such, the transformer's efficiency will be governed by the loss mechanisms (mechanical and electrical) in the piezoceramic. For PZT8,  $Q_M=1000$ , whereas,  $Q_E=250$ , hence it may be seen that the dielectric loss dominates and will be the major contributor to reduced efficiency. Consequently, to facilitate the optimization of piezoelectric transformer designs, the effects of dielectric loss must be included in the design and analysis tools.

In time-domain finite element modeling, frequency characteristics may be extracted by performing a transient calculation and subsequently applying a Fourier transform to obtain the corresponding frequency domain response. However, to avoid employing windowing functions (which may significantly distort the resultant frequency response), the time-domain response must be fully "rung down" before applying the FFT. (In fact, this is one of the main attractions of time-domain analysis since it permits the frequency response across a wide-frequency band to be obtained via a single calculation). If losses are omitted from the analysis, then in the absence of any external mechanical or electrical damping mechanism, the system will continue to

resonate indefinitely, thus preventing the accurate determination of the device's response as a function of frequency.

### DIFFERENT TYPES OF LOSS MECHANISM

There are several loss mechanisms of importance when modeling piezoelectric transduction devices. These include resistive losses in external electronics, radiation loss to the surrounding medium, mechanical and dielectric loss in the piezoceramic and mechanical loss in passive components such as backing, fillers and matching layers.

In terms of a transducer's ring-down, external loss mechanisms will typically tend to dominate the transducer's mechanical response, however, in terms of heat generation within the piezoceramic, dielectric loss often provides the more significant contribution. Although, there is a varying amount of mechanical and dielectric loss in the piezoceramic at all frequencies, the effects are more significant at some frequencies than at others. Dielectric loss will typically increase a transducer's resistive component by approximately the same amount at both electrical and mechanical resonance. However, the percentage increase at electrical resonance is far more significant than at the mechanical resonance. Consequently, since a transducer is typically driven at its electrical resonance, the dielectric loss often results in a significant increase in internal losses for a fixed applied voltage. This increase results in a corresponding increase in internal heat generation.

#### Measurement of Mechanical and Dielectric Loss

In transducer models that are based around wave-propagation through multi-layered media, mechanical attenuation is normally quantified in terms an attenuation per unit length,  $\alpha$ . Since  $\alpha$  is specified as a logarithmic quantity (Nepers/m), the resultant mechanical amplitude attenuation is incorporated in the analysis via an " $exp(\alpha x)$ " scalar multiplier. It is often more intuitive to express the mechanical attenuation with units dB/cm @ 1MHz. Under these circumstances,  $\alpha$  may be written as,

$$\alpha = -5 A_{dB1} \frac{f}{10^6} \ln(10) \quad \text{Eqn. 1}$$

where  $f$  is the frequency of interest in Hz, and  $A_{dB1}$  is the attenuation in dB/cm at a frequency of 1MHz.

It may be shown that a constant complex stiffness,  $C$ , with real part  $C'$  and imaginary part  $C''$  produces a linear increase of  $A_{dB}$  with  $f$ .

$A_{dB}$  at a frequency  $f$  may now be written as,

$$A_{dB} = \frac{\pi f}{5 \ln(10) Q_M v} \quad \text{Eqn. 2}$$

Here  $v$  is the wave speed and  $Q_M$  is the mechanical Q defined as follows:

$$Q_M = C' / C'' \quad \text{Eqn. 3}$$

Dielectric loss is typically quantified in terms of a material's dielectric loss tangent,  $\tan \delta_E$  which may be defined as follows,

$$\tan \delta_E = \frac{1}{Q_E} \quad \text{Eqn. 4}$$

where  $Q_E$  is the electrical Q for the material.  $\tan \delta_E$  may also be written in terms of the real,  $\epsilon'$ , and imaginary,  $\epsilon''$ , parts of the material's clamped dielectric constant,  $\epsilon^S$ , as follows,

$$\tan \delta_E = \frac{\epsilon''}{\epsilon'} \quad \text{Eqn. 5}$$

The following table lists text-book [1] values for the mechanical and electrical Q's for some of the more commonly used piezoceramics:

	$Q_M$	$Q_E$
PZT-5A	75	50
PZT-5H	65	50
PZT-8	1000	250

**Table 1:** Mechanical and dielectric Q values

From the above table, it may be seen that in both PZT5A and PZT5H, the dielectric and mechanical loss mechanisms will provide approximately the same degree of energy absorption. However, in materials such as PZT-8, which is often used in high-drive actuator applications and piezoelectric transformers, the dielectric loss is significantly greater (low  $Q_E$ ) than the mechanical loss. Consequently, if optimal efficiency is a design goal, then the dielectric loss mechanism must be included in the analysis tools for improved accuracy.

The Piezoelectric Resonance Analysis Program (PRAP) [2] may be used to extract complex electromechanical material constants via electrical impedance measurements made on a set of IEEE standard resonators [3]. This program determines the material constants based on advanced curve fitting techniques applied to the electrical impedance spectra. However, it is important to note that the actual material constants may be inherently frequency dependent, hence the “extracted” values are only valid at the center frequency which was used by PRAP to determine those particular properties. Higher harmonics may also be used to make additional measurements at other frequencies.

An alternative method, which may be used to determine  $Q_M$  ( $A_{dB}$ ) and  $\tan\delta_E$ , is by adjusting the loss mechanisms in a 1D analytic transducer model until the simulated response agrees with the corresponding experimental measurement. The following equation may be used to determine the electrical impedance,  $Z_T$ , of a 1D thickness mode resonator [4],

$$Z_T = \frac{1}{sC_O} \left[ 1 - \frac{k_T^2}{sT} \left( \frac{\bar{K}_F T_F}{2} + \frac{\bar{K}_B T_B}{2} \right) \right] \quad \text{Eqn. 6}$$

Where,

- $s$  is the Laplacian complex variable
- $T$  is the one-way propagation time
- $C_O$  is the clamped capacitance of the transducer
- $k_T$  is the thickness mode coupling coefficient
- $T_F$  and  $T_B$ , the transmission coefficients from the front and back faces respectively, are given by

$$T_F = 2Z_C / (Z_C + Z_1) \quad \text{Eqn. 7}$$

$$T_B = 2Z_C / (Z_C + Z_2) \quad \text{Eqn. 8}$$

$R_F$  and  $R_B$ , the reflection coefficients from the front and back faces respectively, are given by

$$R_F = (Z_C - Z_1) / (Z_C + Z_1) \quad \text{Eqn. 9}$$

$$R_B = (Z_C - Z_2) / (Z_C + Z_2) \quad \text{Eqn. 10}$$

Finally,  $K_F$  and  $K_B$  are defined as,

$$K_F = \frac{(1 - e^{-sT})(1 - R_B e^{-sT})}{(1 - R_F R_B e^{-2sT})} \quad \text{Eqn. 11}$$

$$K_B = \frac{(1 - e^{-sT})(1 - R_F e^{-sT})}{(1 - R_F R_B e^{-2sT})} \quad \text{Eqn. 12}$$

Using Eqn. 6 and the following steps, it is possible to determine the mechanical and dielectric losses for a piezoceramic thickness mode resonator:

1. Run analytic model with no damping (just radiation losses for operation into air)
2. Adjust  $\epsilon'$  via the real part of admittance
3. Adjust  $Q_M$  by matching the amplitude of the mechanical resonance peaks in the impedance magnitude spectrum
4. Adjust  $\epsilon''$  via the imaginary part of admittance

The same steps could be repeated for the other IEEE resonators to quantify the losses in the other modes. In practice, it is usually just assumed that the loss tangents are the same in each direction.

### TIME & FREQUENCY DOMAIN REPRESENTATION OF LOSS MECHANISMS

In frequency-domain analyses of electromechanical systems, energy absorption is often included by making the stiffness and dielectric constants complex. This permits matching observed frequency dependencies of absorption on a frequency-by-frequency basis. Of course, “complexifying” cannot be done arbitrarily since the real and imaginary parts of a linear system’s frequency-domain response must be conjugate harmonic functions to guarantee causality in the time-domain. When the analysis is performed strictly in the time-domain, prescribed frequency-dependent absorption is more problematic. Nonetheless, linear models based on relaxation mechanisms (standard linear solid), or convenient numerical paradigms (Rayleigh damping) have been widely accepted. By choosing the appropriate model, the prescribed variation of absorption versus frequency can usually be matched over the frequency range of interest.

In the PZFlex finite element code, we have implemented several linear viscoelastic models for mechanical loss. These are described in [5]. The mechanical viscoelastic models have analogs that can be used to account for dielectric losses. For example, the standard linear solid in the mechanics literature is the same mathematical expression as Debye relaxation used to model dielectric loss. Table 2 lists the time and frequency domain relations for each model. These expressions are given in 1D for simplicity. The results correspond to one entry in the second order dielectric tensor. Furthermore, we also assume that the dielectric tensor is symmetric. In this case, there is a material

orientation for which it becomes diagonal. We also assume that the principle axes of the real part coincide with the principle axes of the imaginary part. In this case, there are at most 3 independent dielectric functions at any given point.

TIME	FREQUENCY
<i>Simple Loss Model</i>	
$D = \epsilon E + \gamma \dot{E}$	$D = (\epsilon - j\omega\gamma)E$
<i>Simple Loss With Conduction</i>	
$\dot{D} = \epsilon \dot{E} + \gamma \ddot{E} + \sigma E$	$D = (\epsilon - j\omega\gamma + \frac{\sigma}{\omega})E$
<i>Debye Relaxation Model</i>	
$D + \tau \dot{D} = \epsilon_s E + \tau \epsilon_\infty \dot{E}$	$D = \left[ \begin{array}{c} \epsilon_\infty + \frac{(\epsilon_s - \epsilon_\infty)}{(1 + \omega^2 \tau^2)} \\ + j\omega\tau \frac{(\epsilon_s - \epsilon_\infty)}{(1 + \omega^2 \tau^2)} \end{array} \right] E$

**Table 2:** Time-domain dielectric loss models and their frequency-domain counterparts

Experimental results presented in the following section demonstrate that the Debye relaxation model provides a reasonable representation of the dielectric function over a wide frequency range. If better correlation were necessary, multiple mechanism relaxation models provide a means of obtaining it. In fact, this approach has some basis in material science [6]. From an implementation standpoint, each additional mechanism increases the CPU cost and number of storage arrays. At this point, the extra cost is deemed unwarranted.

**PRELIMINARY RESULTS**

Experimental impedance data for a disk of Motorola 3203HD PLZT (0.508mm thick, 10mm diameter) has been used to measure the mechanical and dielectric loss properties for this material. The 1D analytic model and experimental resonator “curve-fitting” technique described earlier was used to determine this material’s mechanical and dielectric loss properties. Furthermore, the PRAP code was also used to measure the loss properties at the resonator’s fundamental resonant frequency and its harmonics.

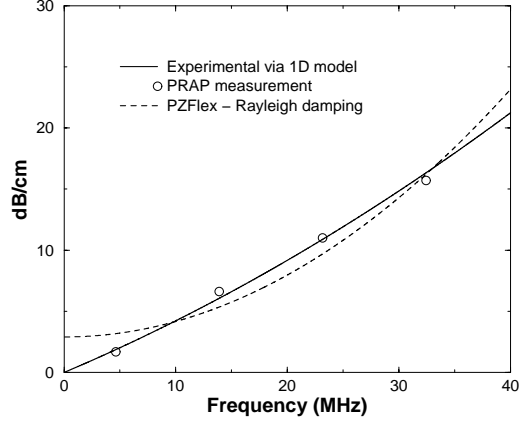


**Figure 1:** Mechanical attenuation (dB/cm) for Motorola 3203HD PLZT

Figure 1 shows the experimental and simulated mechanical attenuation ( $A_{dB}$ ) as a function of frequency. It may be seen that over the entire frequency range, the correlation between experiment is reasonably good. However, for most applications, such a large frequency range is not particularly relevant, but instead there will be a reduced frequency range of primary interest. Under these circumstances, the Rayleigh damping model may be tuned so that it matches the experimental data with much greater accuracy.

It should be noted that the experimental data does not exhibit a perfectly linear variation with frequency (as is often assumed in practice). In fact, it may be shown that assuming a linear dB/cm variation in the frequency domain will result in non-causality in the time domain.

The measured values for  $\epsilon'$  and  $\epsilon''$  are shown in Figures 2 and 3 respectively. These figures also show the dielectric loss function that may be obtained by implementing a Debye model. In addition, the results for a simple loss model, with and without a conductivity term, are also included. Over a wide frequency range (0–40MHz), the Debye model matches the experimental data within 2%. For the more limited frequency ranges employed in a given simulation, even better agreement may be obtained. However, although the simple loss models do not offer such good correlation over an extended frequency range, over a more restricted range, these simpler, easier to implement and faster to compute models, can offer an excellent match. The simple loss model with a conductivity term has been included to illustrate its form, however, due to its low frequency response, it is not a good model for this particular data.

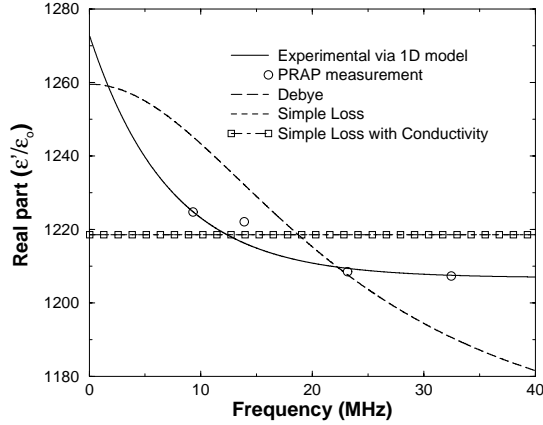


Figure 2:  $\epsilon'/\epsilon_0$  for Motorola 3203HD PLZT

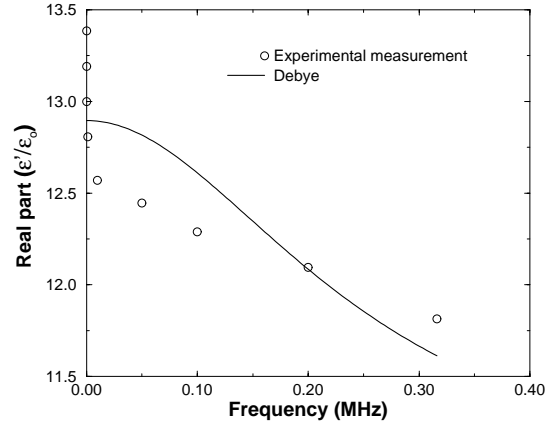


Figure 4:  $\epsilon'/\epsilon_0$  for Kynar-PVDF

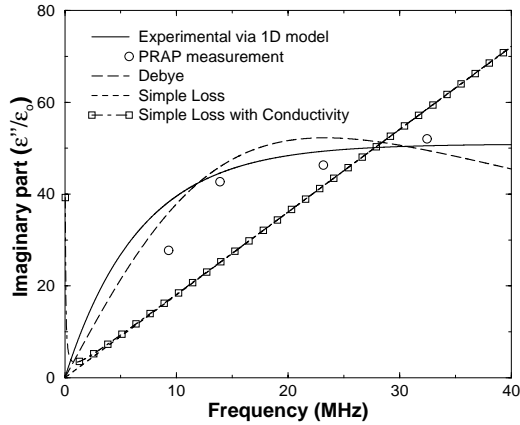


Figure 3:  $\epsilon''/\epsilon_0$  for Motorola 3203HD PLZT

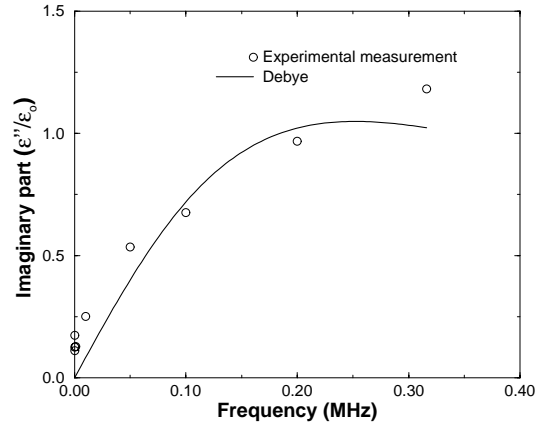


Figure 5:  $\epsilon''/\epsilon_0$  for Kynar-PVDF

Figures 4 and 5 show the real and imaginary parts respectively of the dielectric constant for Kynar PVDF [7]. The experimental data is taken from reference [7] and is cross-plotted against the simulated dielectric loss using a Debye loss model. The simulated dielectric loss is seen to provide a close match with the experimental measurements over the entire frequency range, with a maximum error of about 3% (note the range of y-axis values).

Figure 6 shows the electrical impedance magnitude response for the disk of Motorola 3203HD PLZT. The experimental measurement is cross-plotted against the simulated response curves obtained via the 1D analytic expression from Eqn-6. The 1D model was used to predict the transducer's response with various combinations of loss mechanism included in the model. The mechanical attenuation has the greatest effect on the impedance magnitude, whilst the inclusion of the

dielectric loss mechanism has minimal impact on the impedance magnitude. On the other hand, if we now consider the real (or resistive) part of the device's impedance response (Figure 7), the dielectric loss is seen to have a much more significant impact on overall device performance.

From Figure 6 it may be seen that at even harmonics of the transducer's mechanical resonant frequency ( $2f_M, 4f_M, 6f_M, \dots$ ), the impedance magnitude is nominally independent of mechanical and dielectric loss. At this frequency there is no net displacement on the surface of the transducer, i.e. it is effectively clamped. Consequently, the standard technique for measuring  $\epsilon^S$  based on the impedance at  $2f_M$  (or any other even harmonic) is seen to be justifiable. However, since the real impedance (Figure 7) is highly sensitive to all loss mechanisms, not just dielectric loss,  $\tan \delta_E$  can not be determined accurately using the same technique. More

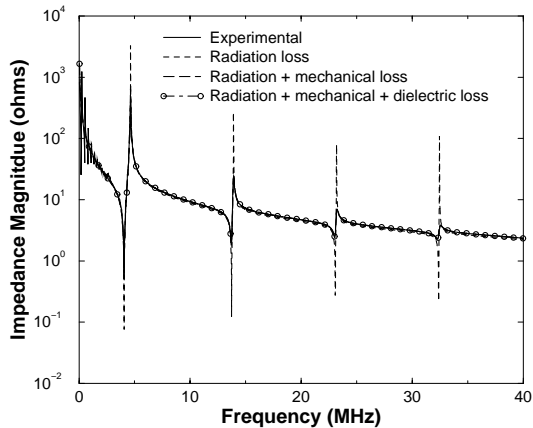


**Figure 6:** Impedance magnitude spectrum for the disk of Motorola 3203HD PLZT

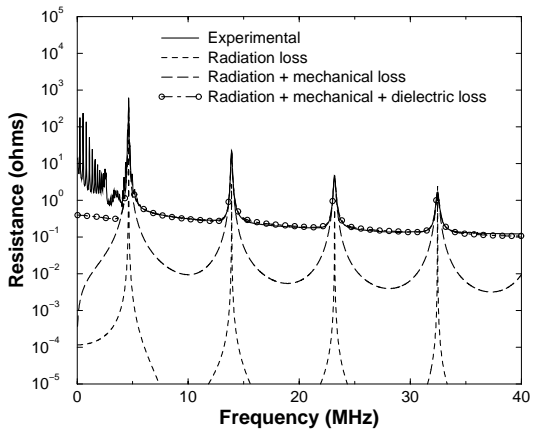


**Figure 7:** Resistive part of the impedance response for the disk of Motorola 3203HD PLZT

accurate measurement over a continuous frequency range is possible using the analytic-experimental approach described in this paper.

### CONCLUSIONS

We have explored the measurement and modeling of material loss mechanisms in two common piezoelectric materials. The goal was to observe the variation in material response with frequency to guide the selection of appropriate, theoretically sound, time domain material models. Though by no means an exhaustive set, we hope that the measured response is at least qualitatively representative of most piezoelectric materials in the frequency range of interest.

A procedure has been proposed for extracting the mechanical and dielectric loss functions for IEEE resonators over a continuous frequency band. The results compare well with the discrete values obtained from PRAP. Based on these results, it appears that a classical Debye relaxation model provides an adequate model for dielectric loss, whilst Rayleigh damping provides an adequate model for mechanical loss.

1D simulations of a thickness mode resonator demonstrate that properly modeling both the mechanical and dielectric losses dramatically improves the ability to calculate the real part of impedance.

Since dielectric losses do not dramatically effect the dynamic response of a device, it may be computationally expedient to simply scale the mechanical and/or electric intensities by the appropriate constants to compute the heat generation.

### ACKNOWLEDGEMENTS

This work was supported in part by DARPA and the Office of Naval Research. The authors would also like to express their gratitude to Professor Binu Mukherjee and Dr Stewart Sherrit from the Royal Military College of Canada for their assistance with experimental measurements and Ron Tasker of TASI Technical Software for facilitating the PRAP analysis.

### REFERENCES

- [1] Kino, G.S., "Acoustic Waves – Devices, Imaging, & Analog Signal Processing", Prentice Hall, 1987
- [2] TASI Technical Software, 174 Montreal Street, Kingston, Ontario, Canada, K7K 3G4
- [3] IEEE Standard on Piezoelectricity, The Institute of Electrical and Electronic Engineers, 1988
- [4] Hayward, G., "A systems feedback representation of piezoelectric transducer operational impedance", *Ultrasonics* (July 1984), pp153-162
- [5] Wojcik, G., J. Mould, F. Lizzi, N. Abboud, M. Ostromogilsky, D. Vaughan, "Nonlinear Modeling of Therapeutic Ultrasound," *Proc. 1995 IEEE Ultrasonics Symposium*, pp. 1617-1622.
- [6] Gerhardt, R., "Causes of Dielectric Dispersion in Ferroelectric Materials," *Advances in Dielectric Ceramic Materials*, *Ceramic Trans.*, Vol 88, pp. 41-60, 1998.
- [7] Kynar Piezo Film, Technical Manual, Pennwalt Corp. Valley Forge, PA, 1987.